Diabetes Exacerbates the Intraocular Pressure-Independent Retinal Ganglion Cells Degeneration in the DBA/2J Model of Glaucoma

Rosario Amato,[1,2] Francesca Lazzara,[2,3] Tsung-Han Chou,[2] Giovanni Luca Romano,[2,3] Maurizio Cammalleri,[1] Massimo Dal Monte,[1] Giovanni Casini,[1] and Vittorio Porciatti[2]

[1]Department of Biology, University of Pisa, Pisa, Italy
[2]Bascom Palmer Eye Institute, Miller School of Medicine, University of Miami, Miami, Florida, United States
[3]Biomedical and Biotechnological Sciences Department, University of Catania, Catania, Italy

PURPOSE. Glaucoma is a multifactorial disease, causing retinal ganglion cells (RGCs) and optic nerve degeneration. The role of diabetes as a risk factor for glaucoma has been postulated but still not unequivocally demonstrated. The purpose of this study is to clarify the effect of diabetes in the early progression of glaucomatous RGC dysfunction preceding intraocular pressure (IOP) elevation, using the DBA/2J mouse (D2) model of glaucoma.

METHODS. D2 mice were injected with streptozotocin (STZ) obtaining a combined model of diabetes and glaucoma (D2 + STZ). D2 and D2 + STZ mice were monitored for weight, glycemia, and IOP from 3.5 to 6 months of age. In addition, the activity of RGC and outer retina were assessed using pattern electroretinogram (PERG) and flash electroretinogram (FERG), respectively. At the end point, RGC density and astrogliosis were evaluated in flat mounted retinas. In addition, Müller cell reactivity was evaluated in retinal cross-sections. Finally, the expression of inflammation and oxidative stress markers were analyzed.

RESULTS. IOP was not influenced by time or diabetes. In contrast, RGC activity resulted progressively decreased in the D2 group independently from IOP elevation and outer retinal dysfunction. Diabetes exacerbated RGC dysfunction, which resulted independent from variation in IOP and outer retinal activity. Diabetic retinas displayed decreased RGC density and increased glial reactivity given by an increment in oxidative stress and inflammation.

CONCLUSIONS. Diabetes can act as an IOP-independent risk factor for the early progression of glaucoma promoting oxidative stress and inflammation-mediated RGC dysfunction, glial reactivity, and cellular death.

Keywords: pattern electroretinogram, flash electroretinogram, oxidative stress, inflammation

Glaucoma is characterized by a progressive optic neuropathy, including chronic axonal damage and retinal ganglion cell (RGC) loss.[1] Owing to the complex multifactorial nature of glaucoma, the risk factors and molecular mechanisms driving its pathophysiology are still far from being fully elucidated. IOP elevation represents one of the most recurrent risk factors, promoting glaucomatous progression and RGC neurodegeneration.[2] IOP is commonly assessed for the diagnosis and follow-up of glaucoma and its elevation represents the main target for the pharmaceutical treatments in use with significant but not resolutive effects.[3] Noteworthy, IOP elevation is not an overall feature of all glaucoma subgroups because it could manifest later in the progression of the disease or even not occur, as in the case of normotensive glaucoma.[4] These discrepancies highlight the limitations of current glaucoma risk analyses as well as the need of finding further risk factors for the early diagnosis and prognosis of the disease.

In the last years, the almost exclusive IOP-dependent pathophysiological conception has increasingly turned into a comprehensive view of glaucoma, also including the possible role of neuronal dysmetabolism. In effect, RGC display a high metabolic demand to fulfill their role in the visual pathway, thus resulting particularly susceptible to metabolic stress and bioenergetic insufficiency.[5–7] Therefore, pathologies affecting metabolism, such as metabolic syndrome and diabetes, could acquire a key role in glaucoma pathophysiology. Diabetes is known to exert severe detrimental effects on retinal physiology and, in particular, on neural function and viability.[8] Interestingly, several mechanisms driving neurodegeneration in the diabetic retina also result characteristic of glaucoma, such as inflammation, oxidative stress, excitotoxicity, and neurotrophic imbalance. However, although diabetes is a good candidate as a risk factor for glaucoma, clinical and experimental studies have not provided an unquestionable confirmation of its promoting

or contrasting role. In effect, clinical reports showing diabetes as a promoting factor for IOP elevation have been contrasted by other studies disproving any correlation between diabetes and IOP elevation.[9] Similarly, acute diabetes in rats has been shown both to increase RGC apoptosis and, conversely, to delay RGC loss and axonal degeneration after IOP elevation.[10–12]

The role of diabetes as a putative risk factor is likely to be related to glaucoma progression. Thus, it is crucial to test its effects in a model mimicking the dynamics of glaucoma, as is the case of the DBA/2J inherited murine model (D2). D2 mice are characterized by a recessive mutation in the *Gpnmb* and *Tyrp1* genes causing iris atrophy and pigment dispersion, which results in age-dependent development of glaucoma.[13] Typically, D2 mice show IOP elevation, progressive RGC degeneration, optic nerve axon loss, and optic disc excavation starting at 6 months of age (hypertensive stage).[14,15] Interestingly, an early age-dependent loss of RGC activity has been demonstrated before the elevation of IOP at 3 to 6 months of age (normotensive stage).[16] By using the D2 model, it has been demonstrated that diabetes exacerbates the glaucomatous status during the hypertensive stage further increasing IOP at 8.5 months and the relative gliosis.[17] However, it remains unclear whether diabetes influences the glaucomatous RGC loss exclusively through exacerbation of ocular hypertension or if it directly promotes RGC degeneration. In this study, using a longitudinal approach, we investigated the effect of diabetes on glaucoma progression during the D2 model normotensive stage, evaluating time dependent IOP alterations, RGC dysfunction, and outer retinal activity. In addition, the effects of diabetes in D2 mice were analyzed on RGC survival, glial reactivity, and the expression of oxidative stress and inflammatory markers.

MATERIALS AND METHODS

Animals

The study included 20 D2 mice purchased from Jackson Labs (Bar Harbor, ME, USA). All procedures were performed in compliance with the Association for Research in Vision and Ophthalmology (ARVO) statement for use of animals in ophthalmic and vision research. The experimental protocol was approved by the Animal Care and Use Committee of the University of Miami (Project protocol number: 18-182-LF). All mice were maintained in a cyclic light environment (12 hours light: 50 lux – 12 hours: dark) and fed with Grain Based Diet (Lab Diet: 500, Opti-diet; PMI Nutrition International, Inc., Brentwood, MO, USA) and regular water ad libitum. Nonglaucomatous control mice were not considered because the commonly used C57BL/6J or DBA/2J-Gpnmb+/SjJ show some notable differences in inner retinal neural processing that could have a counterpart in the RGC susceptibility to insults or diseases.[18]

Diabetes Induction and Experimental Modeling

Animals were randomly assigned to the glaucomatous control group (D2; $n = 10$) or to the diabetic group (D2 + STZ; $n = 10$). Diabetes was induced at 3.5 months of age by means of daily intraperitoneal injections of streptozotocin (STZ; 50 µg/g body weight) dissolved in sodium citrate buffer (137 mM, pH 4.5) for 5 consecutive days.[19] An equivalent volume of sodium citrate buffer was delivered to the D2 group as glaucoma control. Two weeks after the last injection (4 months of age), the mice were tested for blood glucose levels using a OneTouch Ultra glucometer (LifeScan Inc., Milpitas, CA, USA), and those showing a stable glycemia ≥ 250 mg/dL were considered diabetics.[19] Mice were followed-up for glycemia and weight every 2 weeks, concomitantly with the IOP and electroretinographic recordings. After the last recording session (6 months of age; 2 months of diabetes), the mice were euthanized and the eyes collected for molecular analyses.

IOP Measurement

The mice were anesthetized by intraperitoneal injection (0.5–0.7 mL/kg) of ketamine (42.8 mg/mL) and xylazine (8.6 mg/mL). Five minutes after the induction of anesthesia, each mouse was gently restrained on an adjustable stand and IOP was measured with a rebound tonometer (TonoLab, Colonial Medical Supply, Franconia, NH, USA). The probe tip of the tonometer was aligned with the optical axis of the eye distancing it by 1- to 2-mm. Five consecutive readings were averaged to obtain a reliable measure of the IOP. The eyes were carefully checked for possible damage of the corneal surface due to probe rebound.

Assessment of RGC Function with Pattern Electroretinogram

Immediately after IOP assessment, anesthetized mice were transferred on a custom-made restrainer with a superior incisor bite and ear knobs, which allowed unobstructed visual field. Body temperature was maintained at 37°C using a feedback-controlled heating pad (TCAT-2LV, Physitemp Instruments, Inc., Clifton, NJ, USA). The corneal humidity was preserved with instillation of balanced salt solution eye drops (Alcon Laboratories Inc., Fort Worth, TX, USA). Pupils were undilated and small (<1 mm) to ensure a large depth of focus. Pattern electroretinogram (PERG) assessment was realized using a commercially available PERG system (JÖRVEC, Miami, FL, USA) allowing to record the response from both eyes simultaneously from a stainless-steel needle (Grass, West Warwick, RI, USA) placed in the snout. The reference and ground electrodes were similar needles placed in the medial portion of the scalp and at the root of the tail, respectively. Maximal PERG response was obtained by presenting visual stimuli consisting in black-white horizontal bars (0.05 cycles/deg, 98% contrast) alternating at slightly different frequencies around 1 Hz (right eye, 1.016 Hz; left eye, 1.008 Hz) generated on two light-emitting diode tablets (15 × 15 cm square field, 800 cd/m² mean luminance) and presented independently to each eye at 10 cm distance. Independent PERG signals from each eye were retrieved using one channel continuous acquisition and phase-locking average over 372 epochs for each eye. PERG responses were analyzed by detecting the early positive inflection point (N1), the positive peak (P1), and the belated negative trough (N2) in the PERG waveform. Considering that the amplitudes of the positive (N1-P1) and the negative (P1-N2) components of the PERG response are classically proportional in DBA/2J mice and resulted proportionally affected by STZ (see Supplementary Fig. S1), we preferred to consider the wider P1-N2 amplitude (hereinafter referred as PERG amplitude) to ensure a higher dynamic range of measures, as previously reported.[16,20] PERG recordings were

realized every 2 weeks starting from the baseline corresponding to 3.5 months of age up to the end point at 6 months of age, corresponding to 2 months of diabetes.

Assessment of Outer Retinal Activity using Flash Electroretinogram

Flash electroretinogram (FERG) was recorded as a measure of the outer retinal activity corresponding to the RGC function assessed with PERG, as previously described.[15] Immediately after the PERG recording session, anesthesia was extended by delivering a redosing injection corresponding to 25% of the initial dose. The mouse was then transferred in a new custom restrainer equipped with two micromanipulators holding 0.25 mm diameter silver wire corneal electrodes (World Precision Instruments, Sarasota, FL, USA) configured to a semicircular loop of 2 mm radius. Corneal electrodes were gently placed on the corneal surface avoiding any interference to the visual field. Two subcutaneous stainless-steel needle (Grass, West Warwick, RI, USA) inserted into the scalp midline and the tail root, were used as common reference and ground electrodes, respectively. Visual stimuli consisted of 20 cd/m² mean luminance flash superimposed on a steady background light (12 cd/m² mean luminance) presented within a Ganzfeld bowl. Responses deriving from a total of 60 stimuli were averaged to reduce the influence of the noise on the FERG signal. Averaged FERG waveforms were analyzed with SigmaPlot version 11 software (Systat Software Inc., San Jose, CA, USA), to automatically identify the major positive and negative peaks.

The covariation of FERG corresponding to the PERG response was assessed by considering the overall FERG peak-to-trough amplitude (hereinafter referred as FERG amplitude), in order to effectively include any glaucoma or diabetes-induced changes in both positive and negative components of FERG, not often reliably discernible.[15] A separated analysis of the FERG a-wave, b-wave, and PhNR was performed to analyze the possible contribution of receptoral and post-receptoral activity in the FERG amplitude modulation. In addition, the FERG waveform time-to-peak (FERG latency) was also examined. The temporal resolution of the FERG longitudinal analysis (one recording every 4 weeks starting at 4 months of age up to 6 months of age) was kept lower than the PERG (one recording every 2 weeks starting at 3.5 months of age) for the need of containing the detrimental effect of the anesthesia redosing on the viability of mice.

Immunofluorescence Staining

Mice were transcardially perfused with 4% w/v paraformaldehyde (PFA) dissolved in phosphate-buffered saline (PBS) 0.1 M pH 7.4. Hereafter, eyeballs were enucleated and postfixed by immersion in the same PFA solution for 2 hours at room temperature and then stored at 4°C in 30% w/v sucrose solution in PBS. For whole-mount immunostaining, right and left retinas from four mice per group were dissected and rinsed in PBS before being alternatively incubated with a Guinea Pig polyclonal antibody directed to RNA binding protein multiple splicing (RBPMS; dilution 1:100; ABN1376 Merck KGaA, Darmstadt, Germany) or with a Rabbit monoclonal antibody directed to glial fibrillary acidic protein (GFAP, dilution 1:400; ab207165; Abcam, Cambridge, United Kingdom) diluted in

PBS containing 2% v/v Triton X-100 for 72 hours at 4°C. Hence, retinas were washed in PBS and incubated with secondary antibodies Fluorescein-conjugated Donkey anti-Guinea Pig (dilution 1:80, AP193F; Merck KGaA, Darmstadt, Germany) and AF488-conjugated goat anti-Rabbit (dilution 1:400, ab150077; Abcam, Cambridge, UK). Finally, retinas were rinsed in PBS, flat mounted on polarized glass slides, and coverslipped with a mounting medium (ab104139; Abcam, Cambridge, United Kingdom).

For cross-section immunostaining, four fixed eyecups deriving from two mice per group were embedded in cryogel and frozen using liquid nitrogen. The 10 μm thick coronal sections of the retina were obtained using a cryostat, mounted onto polarized slides, and stored at −20°C until use. The sections were incubated overnight at 4°C with the Rabbit monoclonal antibody against GFAP (1:400) and then with the AF488-conjugated goat anti-Rabbit (1:400) for 2 hours at room temperature, both diluted in PBS containing 0.1% v/v Triton X-100.

Quantitative Analysis of Immunofluorescence Images

Images of both whole-mounted retinas and cross-sections were acquired using an epifluorescence microscope (Ni-E; Nikon-Europe, Amsterdam, The Netherlands) equipped with a digital camera (DS-Fi1c; Nikon-Europe). The analysis of RBPMS-positive RGC density was performed as previously described.[21] Briefly, whole-mounted retinas were sampled at two different radial eccentricities (center = 0.5 mm, periphery = 1.5 mm from the optic disc), and RBPMS positive cells were blindly counted in a total of eight sampling fields (433 × 325 μm). RGC densities were calculated separately in central and peripheral areas by dividing the number of RBPMS positive cells by the field area. The same sampling procedures were adopted for the quantification of the GFAP immunofluorescence density for the astrocytic activation. Then, the images were normalized to background and processed for the measure of mean gray levels using Fiji-ImageJ software.

Quantitative Real-Time PCR

For gene expression analysis, each mouse was euthanized by cervical dislocation and both eyes were enucleated. The deriving retinas were dissected, pooled in a single sample, and stored at −80°C. Total RNA was purified from four independent samples per group using TRIzol Reagent kit (cat. 15596026 ThermoFisher Scientific, Waltham, MA, USA) according to the manufacturer instructions. After spectrophotometric quantification, first-strand cDNA was obtained from 1 μg of total RNA using QuantiTect Reverse Transcription Kit (cat. no. 205310; Qiagen, Hilden, Germany). Quantitative real-time PCR (qPCR) was performed using SsoAdvanced Universal SYBR Green Supermix on a CFX Connect Real-Time PCR Detection System and software CFX manager (Bio-Rad Laboratories, Hercules, CA, USA). Primer sets were designed to hybridize to unique regions of oxidative stress- and inflammation-related genes target sequences displayed in the Table. Target genes were concurrently analyzed with *Rpl13a* as housekeeping gene as it is constitutively expressed for ribosomal protein L13A. The relative threshold cycle (Ct method) was used for comparison with the D2 group.

TABLE. RT-PCR Primer Sequences

Gene	Forward Primer (5′-3′)	Reverse Primer (5′-3′)
Heme oxygenase-1 (HO-1)	AAGCCGAGAATGCTGAGTTCA	GCCGTGTAGATATGGTACAAGGA
Superoxide dismutase 2 (SOD-2)	CAGACCTGCCTTACGACTATGG	CTCGGTGGCGTTGAGATTGTT
Interleukin 6 (IL-6)	GCCTTCCCTACTTCACAAGTC	AGTGCATCATCGTTGTTCATAC
Tumor necrosis factor alpha (TNF-α)	GCCTCTTCTCATTCCTGCTTG	CACTTGGTGGTTTGCTACGAC
Interleukin 10 (IL-10)	CCAAGCCTTATCGGAAATGA	TTTTCACAGGGGAGAAATCG
Ribosomal protein L13A (Rpl13a)	CACTCTGGAGGAGAAACGGAAGG	GCAGGCATGAGGCAAACAGTC

Statistical Analysis

Data were tested for normal distribution using the Shapiro–Wilk test. For the longitudinal analysis, the effect of categorical variables (time and STZ treatment) on single-variable analyses was tested with RM-ANOVA. The generalized estimating equation (GEE) approach was instead used to analyze the effect of categorical variables on the correlation between primary continuous variables (IOP and PERG amplitude) and influencing covariates. The GEE included measures retrieved from both eyes while accounting for both the within-subject (right and left eye) and between-subject differences over a 10 mice per group. For end point analyses, unpaired *t*-test or 2-way ANOVA with Bonferroni post hoc test were appropriately used to test the effect of a single categorical variable or two categorical variables, respectively. Relevant data were graphically displayed and statistically analyzed with JMP Pro 14.2 (SAS Institute Inc., Cary, NC, USA) and IBM SPSS statistics (IBM, Armonk, NY, USA). Data are expressed as mean ± SEM of the reported n values. Differences with $P < 0.05$ were considered significant.

RESULTS

Diabetes Onset and Time-Dependent Effects on IOP Variation

To assess the onset and maintenance of the diabetic condition, we tested the glycemia in D2 and D2 + STZ groups biweekly starting at 3.5 months of age, before diabetes induction, up to the end point at 6 months of age (Fig. 1A). Mice belonging to both experimental groups showed similar blood glucose levels and weight before diabetes induction (*t*-test $P = 0.98$, and $P = 0.99$, respectively). The treatment with STZ produced an increase in glycemia in the D2 + STZ group compared with D2 (RM-ANOVA $P < 0.0001$), which, starting at 4 months of age, resulted continuatively higher than the cutoff value settled at 250 mg/dL up to the end point of the protocol. As a further evidence of the diabetic condition, mice subjected to the treatment with STZ displayed a significant decrease of the age-dependent gain of weight compared to D2 control mice (RM-ANOVA time $P = 0.0074$, STZ $P = 0.0204$; Fig. 1B). Considering glycemia and weight as systemic covariates dynamically describing the diabetic status, we tested the effect of diabetes on IOP variations over the follow-up period (Fig. 1C). The GEE analysis revealed that both D2 and D2 + STZ mice displayed a mild decrease in IOP (∼1 mm Hg; GEE time $P = 0.022$) over the period under investigation. In this context, the STZ-treated group showed slightly higher IOP (∼2 mm Hg) compared to D2 (GEE STZ $P = 0.003$), maintained along the follow-up period (GEE interaction $P = 0.609$).
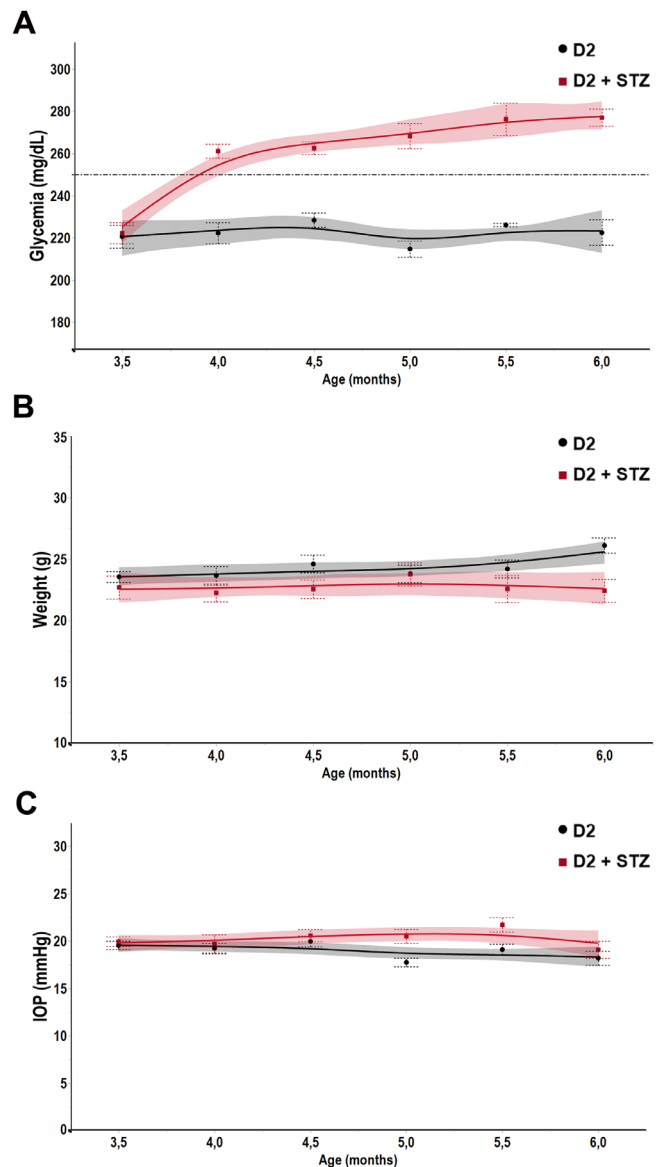

FIGURE 1. Longitudinal evaluation of glycemia (**A**) and weight (**B**) as parameters describing the progressive diabetic status in D2 (*black dots*) and D2 + STZ (*red squares*) mice. Data are expressed as mean ± SEM of $n = 10$ mice per group, spline-fitted (*continuous line*) with 95% confidence interval (*fading area*) and analyzed using RM-ANOVA. (**C**) Longitudinal assessment of individual IOP variations. Data are expressed as mean ± SEM of $n = 10$, and spline-fitted with 95% confidence interval (*fading area*). Data were analyzed using GEE including the effect of glycemia and weight as covariates.
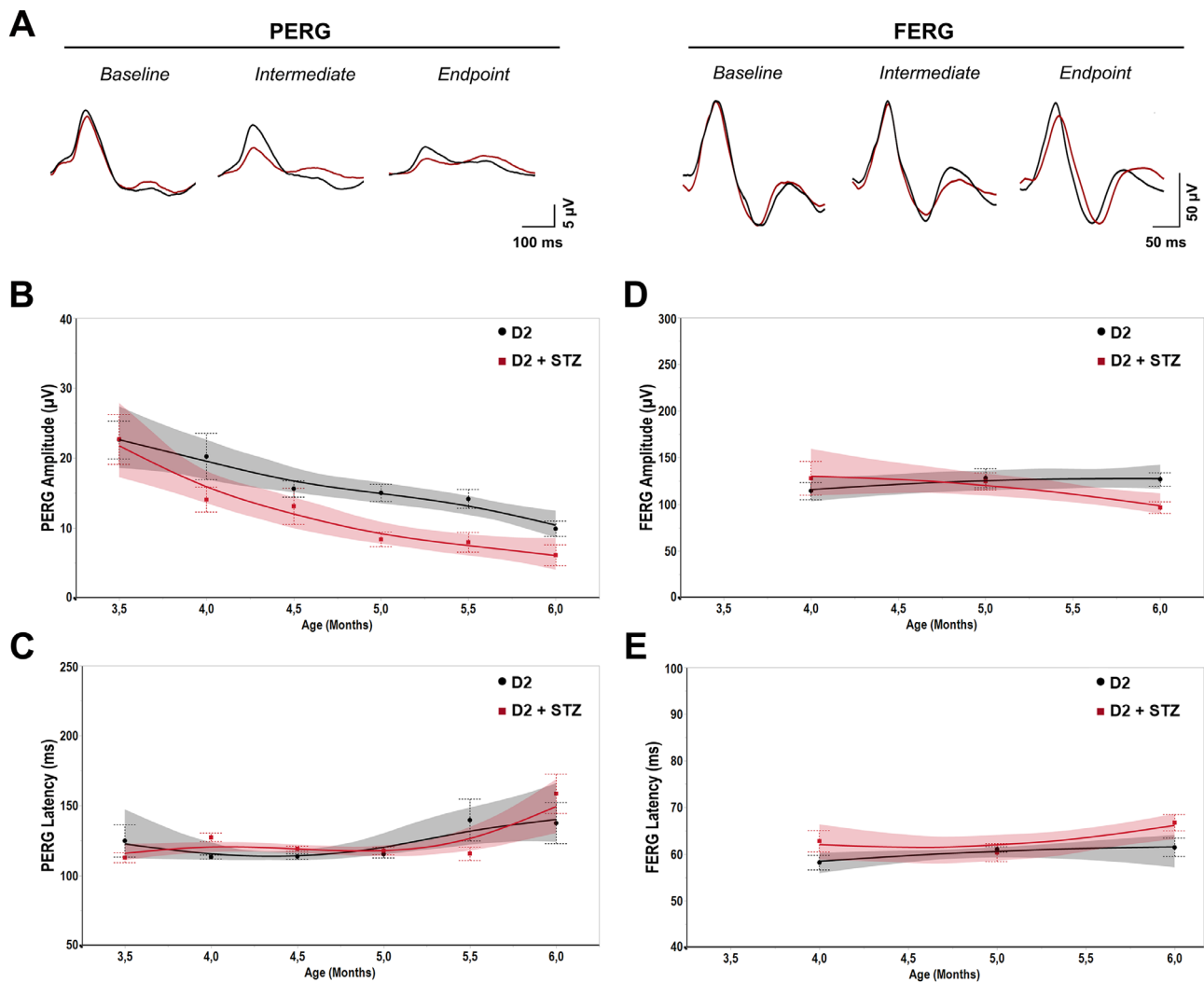
FIGURE 2. Longitudinal analysis of time-dependent variations in RGC activity measured with PERG and relative outer retinal activity using FERG. (**A**) Representative PERG and FERG waveforms of D2 (*black*) and D2 + STZ (*red*) mice deriving from baseline, intermediate, and end point recordings during the analyzed time-window. (**B, C**) Follow-up of PERG response over-time through the assessment of PERG amplitude and PERG latency in both groups. (**D, E**) Longitudinal assessment of FERG amplitude and FERG latency. Data are expressed as mean ± SEM of $n = 10$, considering the average of individual mice contralateral eyes recordings, and spline-fitted with 95% confidence interval (*fading area*). PERG response was analyzed using GEE including IOP and FERG response parameters as covariates.

Longitudinal Multivariate Analysis of Diabetes Effects on RGC Activity

Longitudinal variations in RGC and outer retinal activities were assessed in D2 and D2 + STZ mice with PERG and FERG recordings, whose representative waveforms are displayed in Fig. 2A. Considering PERG amplitude as a sensitive parameter related with RGC activity, we evaluated the effect of age and diabetes using the GEE integrated model incorporating the influence of the corresponding PERG latency, IOP, and FERG parameters as covariates. PERG amplitude resulted significantly influenced by age in both groups, displaying a time-consistent decrease during the period under analysis (Fig. 2B). The effect of age on PERG amplitude was independent from the relative PERG latency, which was constant in both groups (Fig. 2C), and from individual covariations of IOP (see Fig. 1C), FERG amplitude (Fig. 2D) and FERG latency (Fig. 2E; GEE time *P* = 0.003). The time-dependent decrease of PERG amplitude resulted significantly different between D2 and D2 + STZ

mice (GEE estimated marginal means D2 = 15.26 ± 2.03 µV, D2 + STZ = 7.80 ± 0.97 µV), continuously along the follow-up period (GEE interaction *P* = 0.538). Interestingly, the D2 + STZ group also displayed a slight decrease in the overall FERG amplitude occurring exclusively at 6 months of age compared to the D2 group (30,04 ± 13,14 µV, RM-ANOVA *P* < 0.0415), which mainly corresponded to the alteration of the b-wave (see Supplementary Fig. S2). However, although the D2 + STZ group displayed a covariation of IOP and FERG amplitude compared to the D2 group, the effect of diabetes on PERG amplitude appeared to be anticipated and not proportional, thus resulting independent from the influence of covariates (GEE STZ *P* = 0.001).

Effect of Diabetes on RGC Density and Gliotic Activity

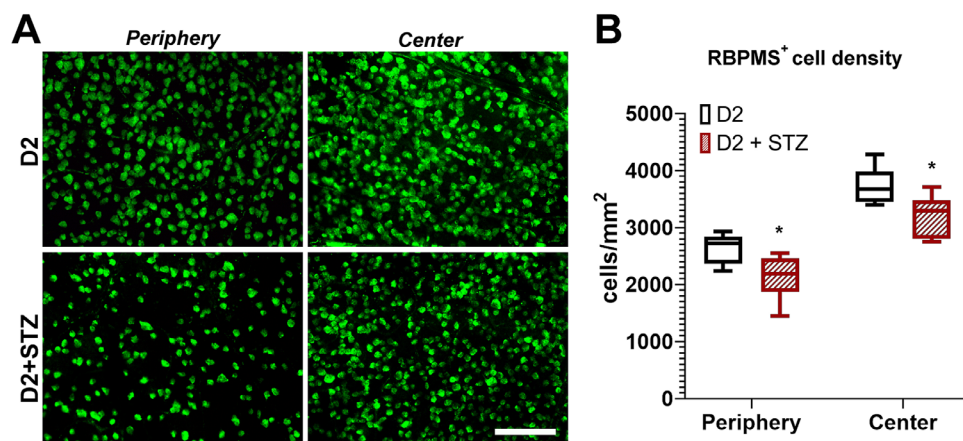The integrated effect of glaucoma and diabetes on RGC density was evaluated at the follow-up endpoint by perform-

FIGURE 3. Immunofluorescence staining of RBPMS positive cells for the analysis of RGC density. (**A**) Representative images of RBPMS staining in peripheral and central areas of D2 and D2 + STZ mice retinas at the follow-up end point. Scale bar 100 μm. (**B**) Analysis of RBPMS-positive cell density in D2 (*black box*) and D2 + STZ (*red box*) groups, differentially sampled from the peripheral and central areas of the retina. Data derive from the average of four radial opposite sampling sites per area in each retina. Box plots describe the statistical distribution of $n = 4$ independent retinas. Data were analyzed using 2-way ANOVA with Bonferroni post hoc test. *$P < 0.05$.

ing a quantitative analysis of RBPMS immunopositive cells (Fig. 3). The D2 group showed a typical difference in RGC density between periphery (2627 ± 119.21 cells/mm²; see Fig. 3A) and center (3707 ± 154.62 cells/mm²; 2-way ANOVA $P = 0.002$; Fig. 3B). The RGC density in D2 + STZ mice was significantly lower in both central (3201,78 ± 128,56 cells/mm²; Fig. 3C) and peripheral (2129.46 ± 38.90 cells/mm²; Fig. 3D) areas of the retina compared to D2 group (2-way ANOVA $P < 0.0001$). The effect of diabetes on the RGC density was similar in the two areas of the retina because the amount of cell loss was comparable (periphery = -18.9 ± 9.4 %; center = -13.6 ± 6.3%; 2-way ANOVA interaction $P = 0.9788$; Fig. 3E). Concomitantly to the analysis of RGC density, we evaluated the gliotic status of astrocytes in whole-mount retinas performing a morphological analysis and a densitometric quantification of the GFAP immunostaining (Fig. 4). Astrocytes in D2 mice retinas showed a typical inactive phenotype with well-organized and thin branching processes (see Fig. 4A). Contrariwise, D2 + STZ mice retinas showed reactive astrocytes characterized by hypertrophic processes forming prominent and poorly organized branching (Fig. 4B). The densitometric analysis revealed a significant increase of GFAP immunofluorescence in D2 + STZ mice compared with D2 mice retinas (+56.7 ± 17.2%, *t*-test $P = 0.0026$; Fig. 4C). The analysis of GFAP-immunostained sections revealed the distribution of the marker along processes across the retinal thickness typically associated to activated Müller cells in both the D2 and the D2 + STZ groups. However, the GFAP immunostaining pattern in the D2 group was associated to small profiles confined to the inner plexiform layer and inner nuclear layer (Fig. 4D), whereas the D2 + STZ mice retinas showed a more prominent GFAP immunoreactivity in the inner retina with processes of Müller cells entering the outer nuclear layer (Fig. 4E).

Expression of Oxidative Stress- and Inflammation-Related Genes

Because most of the pathological mechanisms shared by glaucoma and diabetes are based on oxidative stress and
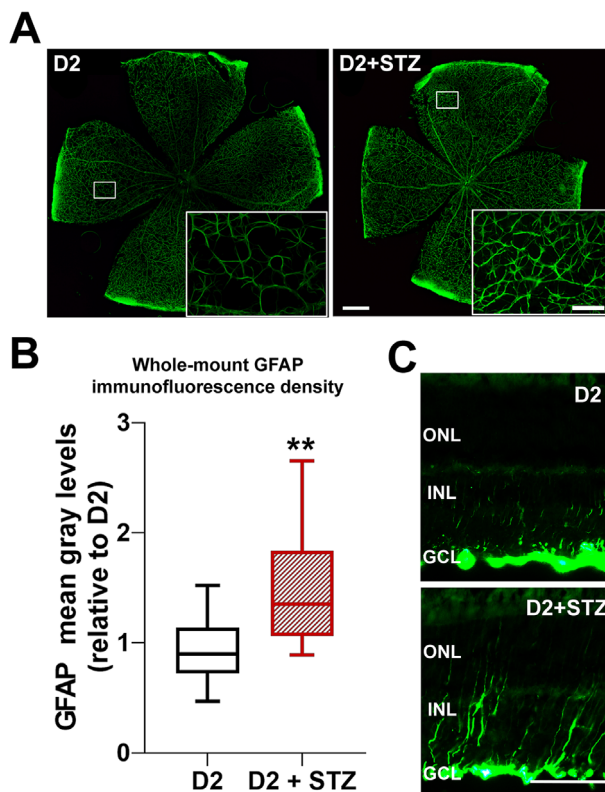

FIGURE 4. GFAP immunostaining in whole-mount retinas and retinal cross-sections for the analysis of astrocytes and Müller cells reactivity at the follow-up end point. (**A**) Representative images of whole-mount retina of D2 and D2 + STZ mice immunostained for GFAP showing retinal astrocytes. Scale bar 500 μm. Insets show higher magnifications of boxed areas for the evaluation of astrocyte morphology and branching. Scale bar 100 μm. (**B**) Densitometric analysis of GFAP immunostaining in D2 (*black box*) and D2 + STZ mice (*red box*). Mean gray levels derive from the average of four radial opposite sampling sites per area in each retina. Box plots describe the statistical distribution of $n = 4$ independent retinas. Data were normalized for D2 group and analyzed using two-tailed *t*-test. **$P < 0.01$. (**C**) Representative images of GFAP immunostaining in retinal cross- section of D2 and D2 + STZ mice retinas highlighting activated Müller cells. Scale bar 100 μm.
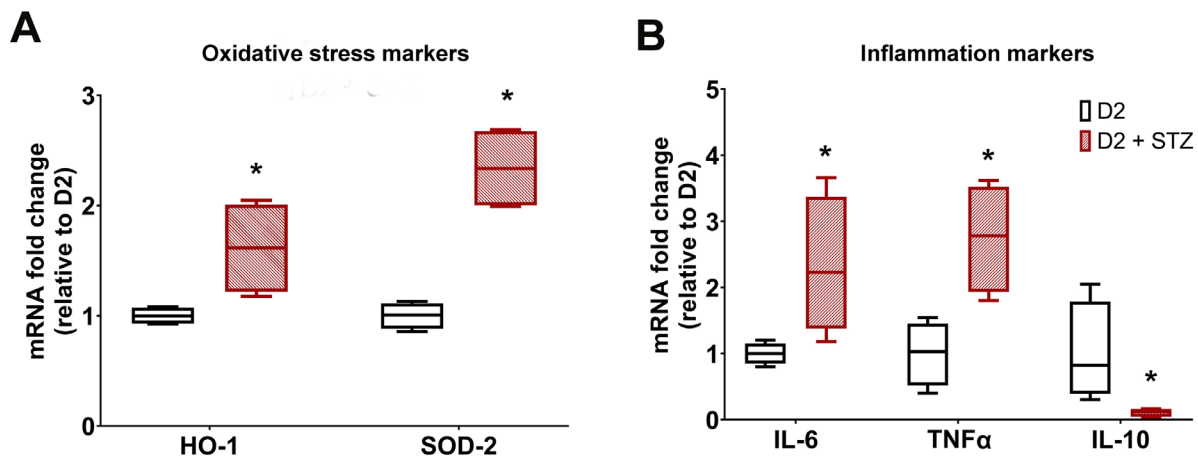
FIGURE 5. Quantitative analysis of the expression of oxidative stress (HO-1 and SOD-2) (**A**) and inflammation-related (IL-6, TNFα, and IL-10) (**B**) markers in D2 (*black box*) and D2 + STZ mice (*red box*) retinas at the follow-up end point. Box plots describe the statistical distribution of $n = 4$ independent retinas. Differences between groups were tested using two-tailed *t*-test. *$P < 0.05$.

inflammation, we tested the difference in related genes expression between experimental groups. The modulation of oxidative stress pathways was evaluated by quantifying the relative expression of HO-1 and SOD-2 (Fig. 5A) in D2 and D2 + STZ mice retinas. The expressions of both markers were significantly increased in the D2 + STZ group compared to the D2 group (HO-1 +74.8 ± 28.9%, *t*-test $P = 0.024$; SOD-2 +133.9 ± 34.9%, *t*-test $P = 0.0044$). The inflammatory status was evaluated by quantifying the relative expression of IL-6 and TNFα as pro-inflammatory and IL-10 as anti-inflammatory cytokines (Fig. 5B). The expressions of both pro-inflammatory cytokines were markedly increased in the D2 + STZ group compared with the D2 group (IL-6 +132.5 ± 52.0%, t-test $P = 0.022$; TNFα +174.6 ± 41.5%; *t*-test $P = 0.011$). Contrariwise, the anti-inflammatory cytokine IL-10 was markedly decreased in the D2 + STZ group compared with the D2 group (-89.3 ± 3%; *t*-test $P = 0.028$).

DISCUSSION

In the present study, we evaluated the role of diabetes as a risk factor for early progression of glaucoma by using a combined model of STZ-induced diabetes in the D2 murine model of glaucoma. In particular, we focused on the early progression of RGC degeneration occurring in D2 mice during the prehypertensive condition between 3 and 6 months of age. Our results demonstrate that diabetes accelerates the longitudinal RGC dysfunction independent from alterations of IOP levels or outer retinal activity and promotes the early loss of RGC density. Our data suggest that diabetes acts as a metabolic stressor further stimulating the oxidative stress and inflammatory mechanisms involving neurons and glia.

Diabetes Does Not Induce a Time-Consistent IOP Elevation in Normotensive Conditions

Classically, IOP elevation has been considered as the driving risk factor for RGC degeneration associated to glaucoma. Indeed, the correlation between IOP and risk/severity of glaucoma has been widely documented by numerous epidemiological studies and experimental reports.[22-24] Diabetes itself has been shown to potentially influence

IOP levels through the alteration of the trabecular meshwork integrity and the vascular properties of the ocular outflow system.[25] However, clinical findings have not stated an unequivocal effect of diabetes on patients' IOP levels because the comparison of different studies has often given controversial results owing to varying diagnostic parameters, assessment criteria, and statistical approaches.[9] Important insights in the study of risk factors and possible treatment strategies influencing IOP levels have derived from the D2 mouse model, because it provides a dynamic and controlled reproduction of progressive IOP-related pathophysiology.[26] D2 mice display a progressive IOP elevation starting at 6 months of age, which correlates with RGC and optic nerve damage.[27] Using this model, Soto and colleagues have shown that the diabetic status promotes the further increase of IOP during the hypertensive stage between 6 and 8.5 months of age.[17] Because it is evident that diabetes positively influences IOP in hypertensive conditions, we focused on the effect of diabetes in the prehypertensive age-frame in order to assess whether diabetes itself could trigger the increase of IOP and therefore anticipate the onset of ocular hypertension. Evaluating the individual IOP variations from 3.5 to 6 months of age, our data display slightly higher IOP levels in the diabetic group compared to the D2 control group. However, the overall magnitude of the increase (2 mm Hg) and the absence of any time-consistent elevation of IOP suggest that this difference is unlikely to result in a significant biological effect. Therefore, the combination of our data with the evidence in literature suggests that, in normotensive condition, the effect of diabetes itself is not sufficient to anticipate a significant time-dependent elevation of IOP, even in glaucoma risk condition. However, considering the potential role of diabetes in the alteration of ocular outflow, diabetes is likely to further integrate the pathophysiological phenomena in hypertensive conditions, thus acting as an exacerbating factor for the IOP elevation.

Diabetes Accelerates the Normotensive RGC Dysfunction Independent from Alterations in IOP and Outer Retinal Activity

Although cases of ocular hypertension often result in progressive neuropathy, RGC degeneration does not depend

necessarily on IOP elevation. For instance, a significant number of cases of glaucomatous neuropathy occur in normotensive conditions (normotensive glaucoma) with RGC degenerative phenomena comparable with those typical of hypertensive glaucoma.[28] Evidence of IOP-independent RGC suffering have also been demonstrated in D2 mice, displaying a significant loss in PERG amplitude in normotensive conditions between 3 and 6 months of age.[16] In addition, the pharmacological or surgical treatment of IOP elevation in cases of hypertensive glaucoma does not result necessarily in a significant protection of RGC.[29] Thus, it is increasingly clear that the view of an almost exclusive role of IOP in the progression of glaucoma is limited and needs to integrate other IOP-independent risk factors and molecular mechanisms cooperating to provoke RGC degeneration. In this context, we tested the possibility that diabetes at this stage could affect RGC integrity via IOP-independent mechanisms. The longitudinal analysis of the PERG response confirms an early age-related RGC dysfunction in D2 mice occurring independent from IOP alterations or outer retinal activity. Interestingly, the RGC dysfunction at this stage results further promoted by diabetes, as demonstrated by the increased loss of PERG amplitude recorded in D2 + STZ mice. Notably, the latter displayed also the alteration of the overall FERG amplitude mainly given by the decrease in the ON bipolar cells-deriving b-wave, demonstrating the detrimental effect of diabetes on the outer neurons activity, in agreement with previous reports.[19] However, because the individual FERG response covariation over time appears delayed and not proportional to PERG alterations, the contribution of the diabetes-induced outer retinal dysfunction to the alteration in RGC activity does not seem to be significant in the time window under investigation, Therefore, our data suggest that, in early glaucoma, the effect of diabetes on RGC activity can be attributed to a direct influence and not to indirect effects involving IOP or outer retinal activity.

Diabetes Reduces the Time-lag Between RGC Dysfunction and Loss Exacerbating Oxidative Stress and Inflammatory Mechanisms

The IOP-independent RGC dysfunction occurring at early stages in D2 mice has been shown to represent a manifestation of the cell suffering preceding a discrete RGC loss.[15,30] In effect, a significant decrease in the RGC density is classically evident around 12 months of age in D2 mice, resulting delayed compared with the typical onset of RGC dysfunctions.[31] The time lag between RGC dysfunction and death in glaucoma has been proposed to derive from the activation of adaptive mechanisms attempting to maintain cell survival in the face of diminished activity under prolonged exposure to stressors. Thus, the possibility to identify and contrast early cellular dysfunctions at this stage has been highlighted as a putative reversibility time window to achieve a significant delay of glaucoma progression.[32] Interestingly, our data show that diabetes in D2 mice produces a significant decrease in RGC density at 6 months of age, corresponding to 2 months of diabetes, compared to the D2 control group. Therefore, besides accelerating the early loss of RGC activity, diabetes significantly affects the cellular viability, thus promoting a possible anticipation of RGC loss. Notably, the combination of diabetes-driven acceleration of the progressive RGC dysfunction and the anticipation of the RGC loss in the early glaucoma could result in the reduction of the

possible intervention time-window, limiting the early diagnosis and aggravating the prognosis of the disease. The RGC vulnerability at the base of the cellular loss of activity and viability in glaucoma has been shown to derive from metabolic stresses possibly due to genetic and/or environmental factors.[7,33,34] Indeed, several aging-like molecular mechanisms could perturbate the RGC metabolic equilibrium promoting oxidative stress and inflammatory activity and inducing glial reaction.[35,36] Noteworthy, increased oxidative and inflammatory processes have been found in D2 mice since the early progression of RGC dysfunction, before the elevation of IOP, suggesting a possible role of the metabolic stress in the early RGC degeneration.[37,38] Considering this, diabetes could be a good candidate as a metabolic stressor for the glaucomatous RGC degeneration. In effect, oxidative stress and inflammation represent crucial pathological mechanisms by which also high glucose-driven metabolic alterations produce detrimental effects on retinal neurons.[39] As hypothesized, our data suggest that the onset of diabetes could exert detrimental effects on the RGC function and viability by further enhancing the ongoing oxidative and inflammatory processes in D2 mice retinas, as demonstrated by the overexpression of HO-1 and SOD-2, as a typical response to the increased oxidative stress, and by the modulation of cytokines on behalf of promoting pro-inflammatory processes.[36] The diabetes-driven enhancement of these pathological mechanisms is clearly represented also by the analysis of the deriving glial reactivity that we have observed in the form of increase in GFAP expression in astrocytes and Müller cell processes, as a phenomenon typically correlated with oxidative stress and neuroinflammation.[40,41] In particular, the Müller cell reactivity, together with our functional evidence of FERG alterations at 6 months of age, could also remark a belated effect of diabetes on the outer retinal cells that, in the context of early glaucoma, could further enhance the glaucomatous RGC dysfunction and degeneration.

CONCLUSION

This study contributes to the characterization of diabetes as a risk factor for the progression of glaucoma. The effect of diabetes during the normotensive stage in D2 mice reveals the possibility that diabetes represents an important risk factor for RGC degeneration independent from IOP elevation. Diabetes enhances oxidative and inflammatory processes further promoting RGC suffering and reducing the putative reversibility time window of glaucoma.

The present study is limited to a basic research grade whose evaluations are based on experimental models, which could mimic but not fully reproduce the extreme complexity of glaucoma and diabetes in humans. For instance, the onset and the progression of glaucoma in the DBA/2J model differs from humans in several temporal and pathophysiological features. Likewise, the evidence deriving from the STZ model are restricted to the type 1 diabetes mellitus and temporally limited within the mouse lifespan. For this reason, the evidence reported in the present paper needs to be further confirmed by perspective observations in patients with diabetes considering not only alterations in IOP, as already assessed in controversial studies, but also the longitudinal evaluation of RGC activity with PERG, which would allow to consider the possible IOP-independent effects of diabetes in the early progression of glaucoma.

References

1. Davis BM, Crawley L, Pahlitzsch M, Javaid F, Cordeiro MF. Glaucoma: the retina and beyond. *Acta Neuropathol*. 2016;132(6):807–826.

2. Nickells RW, Howell GR, Soto I, John SW. Under pressure: cellular and molecular responses during glaucoma, a common neurodegeneration with axonopathy. *Annu Rev Neurosci*. 2012;35:153–179.

3. Stein JD, Khawaja AP, Weizer JS. Glaucoma in adults-screening, diagnosis, and management: a review. *JAMA*. 2021;325(2):164–174.

4. Harada C, Noro T, Kimura A, Guo X, Namekata K, Nakano T, Harada T. Suppression of oxidative stress as potential therapeutic approach for normal tension glaucoma. *Antioxidants (Basel)*. 2020;9(9):874.

5. Morgan JE. Circulation and axonal transport in the optic nerve. *Eye (Lond)*. 2004;18(11):1089–1095.

6. Wong-Riley MT. Energy metabolism of the visual system. *Eye Brain*. 2010;2:99–116.

7. Inman DM, Harun-Or-Rashid M. Metabolic vulnerability in the neurodegenerative disease glaucoma. *Front Neurosci*. 2017;11:146.

8. Lynch SK, Abràmoff MD. Diabetic retinopathy is a neurodegenerative disorder. *Vision Res*. 2017;139:101–107.

9. Wong VH, Bui BV, Vingrys AJ. Clinical and experimental links between diabetes and glaucoma. *Clin Exp Optom*. 2011;94(1):4–23.

10. Kanamori A, Nakamura M, Mukuno H, Maeda H, Negi A. Diabetes has an additive effect on neural apoptosis in rat retina with chronically elevated intraocular pressure. *Curr Eye Res*. 2004;28(1):47–54.

11. Quigley HA. Can diabetes be good for glaucoma? Why can't we believe our own eyes (or data)? *Arch Ophthalmol*. 2009;127(2):227–229.

12. Ebneter A, Chidlow G, Wood JP, Casson RJ. Protection of retinal ganglion cells and the optic nerve during short-term hyperglycemia in experimental glaucoma. *Arch Ophthalmol*. 2011;129(10):1337–1344.

13. John SW, Smith RS, Savinova OV, et al. Essential iris atrophy, pigment dispersion, and glaucoma in DBA/2J mice. *Invest Ophthalmol Vis Sci*. 1998;39(9):1641.

14. Jakobs TC, Libby RT, Ben Y, John SW, Masland RH. Retinal ganglion cell degeneration is topological but not cell type specific in DBA/2J mice. *J Cell Biol*. 2005;171(2):313–325.

15. Nagaraju M, Saleh M, Porciatti V. IOP-dependent retinal ganglion cell dysfunction in glaucomatous DBA/2J mice. *Invest Ophthalmol Vis Sci*. 2007;48(10):4573–4579.

16. Saleh M, Nagaraju M, Porciatti V. Longitudinal evaluation of retinal ganglion cell function and IOP in the DBA/2J mouse model of glaucoma. *Invest Ophthalmol Vis Sci*. 2007;48(10):4564–4572.

17. Soto I, Howell GR, John CW, Kief JL, Libby RT, John SW. DBA/2J mice are susceptible to diabetic nephropathy and diabetic exacerbation of IOP elevation. *PLoS One*. 2014;9(9):e107291.

18. Porciatti V, Chou TH, Feuer WJ. C57BL/6J, DBA/2J, and DBA/2J. Gpnmb mice have different visual signal processing in the inner retina. *Mol Vis*. 2010;16:2939–2947.

19. Sergeys J, Etienne I, Van Hove I, et al. Longitudinal in vivo characterization of the streptozotocin-induced diabetic mouse model: focus on early inner retinal responses. *Invest Ophthalmol Vis Sci*. 2019;60(2):807–822.

20. Chou TH, Bohorquez J, Toft-Nielsen J, Ozdamar O, Porciatti V. Robust mouse pattern electroretinograms derived simultaneously from each eye using a common snout electrode. *Invest Ophthalmol Vis Sci*. 2014;55(4):2469–2475.

21. Chou TH, Romano GL, Amato R, Porciatti V. Nicotinamide-rich diet in DBA/2J mice preserves retinal ganglion cell metabolic function as assessed by PERG adaptation to flicker. *Nutrients*. 2020;12(7):1910.

22. Bonomi L, Marchini G, Marraffa M, Morbio R. The relationship between intraocular pressure and glaucoma in a defined population. Data from the Egna-Neumarkt Glaucoma Study. *Ophthalmologica*. 2001;215(1):34–38.

23. Morrison JC, Cepurna Ying Guo WO, Johnson EC. Pathophysiology of human glaucomatous optic nerve damage: insights from rodent models of glaucoma. *Exp Eye Res*. 2011;93(2):156–164.

24. Miglior S, Bertuzzi F. Relationship between intraocular pressure and glaucoma onset and progression. *Curr Opin Pharmacol*. 2013;13(1):32–35.

25. Sato T, Roy S. Effect of high glucose on fibronectin expression and cell proliferation in trabecular meshwork cells. *Invest Ophthalmol Vis Sci*. 2002;43(1):170–175.

26. Yang XL, van der Merwe Y, Sims J, et al. Age-related changes in eye, brain and visuomotor behavior in the DBA/2J mouse model of chronic glaucoma. *Sci Rep*. 2018;8(1):4643.

27. Libby RT, Anderson MG, Pang IH, et al. Inherited glaucoma in DBA/2J mice: pertinent disease features for studying the neurodegeneration. *Vis Neurosci*. 2005;22(5):637–648.

28. Killer HE, Pircher A. Normal tension glaucoma: review of current understanding and mechanisms of the pathogenesis. *Eye (Lond)*. 2018;32(5):924–930.

29. Leske MC, Heijl A, Hussein M, et al. Factors for glaucoma progression and the effect of treatment: the early manifest glaucoma trial. *Arch Ophthalmol*. 2003;121(1):48–56.

30. Buckingham BP, Inman DM, Lambert W, et al. Progressive ganglion cell degeneration precedes neuronal loss in a mouse model of glaucoma. *J Neurosci*. 2008;28(11):2735–2744.

31. Danias J, Lee KC, Zamora MF, et al. Quantitative analysis of retinal ganglion cell (RGC) loss in aging DBA/2NNia glaucomatous mice: comparison with RGC loss in aging C57/BL6 mice. *Invest Ophthalmol Vis Sci*. 2003;44(12):5151–5162.

32. Porciatti V, Ventura LM. Retinal ganglion cell functional plasticity and optic neuropathy: a comprehensive model. *J Neuroophthalmol*. 2012;32(4):354–358.

33. Harder JM, Guymer C, Wood JPM, et al. Disturbed glucose and pyruvate metabolism in glaucoma with neuroprotection by pyruvate or rapamycin. *Proc Natl Acad Sci USA*. 2020;117(52):33619–33627.

34. Calkins DJ. Adaptive responses to neurodegenerative stress in glaucoma [published online ahead of print February 25, 2021], *Prog Retin Eye Res*. https://doi.org/10.1016/j.preteyeres.2021.1009653.

35. Edwards G, Lee Y, Kim M, Bhanvadia S, Kim KY, Ju WK. Effect of ubiquinol on glaucomatous neurodegeneration and oxidative stress: studies for retinal ganglion cell survival and/or visual function. *Antioxidants (Basel)*. 2020;9(10):952.

36. Romano GL, Amato R, Lazzara F, et al . P2X7 receptor antagonism preserves retinal ganglion cells in glaucomatous mice. *Biochem Pharmacol*. 2020;180:114199.

37. Inman DM, Lambert WS, Calkins DJ, Horner PJ. α-Lipoic acid antioxidant treatment limits glaucoma-related retinal ganglion cell death and dysfunction. *PLoS One*. 2013;8(6):e65389.

38. Wilson GN, Inman DM, Dengler Crish CM, Smith MA, Crish SD. Early pro-inflammatory cytokine elevations in the DBA/2J mouse model of glaucoma. *J Neuroinflammation*. 2015;12:176. Erratum in: *J Neuroinflammation*. 2015;12:191. Denger-Crish, Christine M [corrected to Dengler Crish, Christine M].

39. Rossino MG, Dal Monte M, Casini G. Relationships between neurodegeneration and vascular damage in diabetic retinopathy. *Front Neurosci*. 2019;13:1172.

40. de Hoz R, Rojas B, Ramírez AI, et al. Retinal macroglial responses in health and disease. *Biomed Res Int*. 2016;2016:2954721.

41. Shin ES, Huang Q, Gurel Z, Sorenson CM, Sheibani N. High glucose alters retinal astrocytes phenotype through increased production of inflammatory cytokines and oxidative stress. *PLoS One*. 2014;9(7):e103148.